Science of the Total Environment 909 (2024) 168536

Contents lists available at ScienceDirect

Science of the Total Environment

journal homepage: www.elsevier.com/locate/scitotenv

Thermal stability and micrdose-based coupling CRISPR/Cas12a biosensor for amplification-free detection of *hgcA* gene in paddy soil

Haorui Cao [a,b], Kang Mao [a,*], Hua Zhang [a,*], Qingqing Wu [a,b], Huangxian Ju [c], Xinbin Feng [a]

[a] State Key Laboratory of Environmental Geochemistry, Institute of Geochemistry, Chinese Academy of Sciences, Guiyang 550081, China
[b] University of Chinese Academy of Sciences, Beijing 100049, China
[c] State Key Laboratory of Analytical Chemistry for Life Science, School of Chemistry and Chemical Engineering, Nanjing University, Nanjing 210023, China

HIGHLIGHTS

- CRISPR/Cas12a-based biosensor for methylmercury biomarker gene hgcA in paddy-soil
- A novel thermal stable Cas12a subtype work in 37–57 °C with high efficiency
- Microdose on the detection performance of CRISPR/Cas12a biosensor was discussed.
- Coupling gRNAs obviously increase fluorescence and lower LOD due to synergistic effect.

GRAPHICAL ABSTRACT

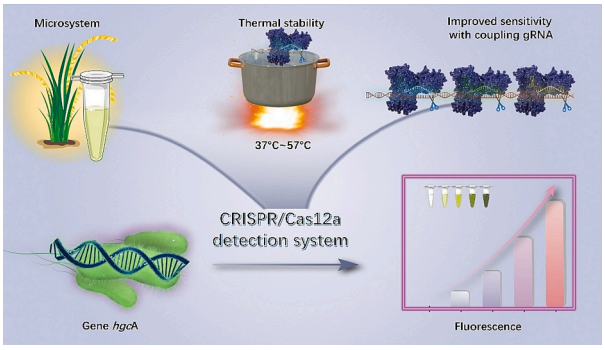

ARTICLE INFO

Editor: Kevin V. Thomas

Keywords:
Methylmercury
CRISPR/Cas12a
HgcA
Paddy soil
Point of use

ABSTRACT

The lack of point-of-use (POU) methods hinders the utilization of the *hgcA* gene to rapidly evaluate methylmercury risks. CRISPR/Cas12a is a promising technology, but shortcomings such as low sensitivity, a strict reaction temperature and high background signal limit its further utilization. Here, a thermally stable microsystem-based CRISPR/Cas12a biosensor was constructed to achieve POU analysis for *hgcA*. First, three target gRNAs were designed to recognize *hgcA*. Then, a microsystem was developed to eliminate the background signal. Next, the effect of temperature on the activity of the Cas12a-gRNA complex was explored and its thermal stability was discovered. After that, coupling gRNA assay was introduced to improve sensitivity, exhibiting a limit of detection as low as 0.49 pM with a linear range of 0.98–125 pM, and a recovery rate between 90 and 110 % for *hgcA*. The biosensor was finally utilized to assess *hgcA* abundance in paddy soil, and high abundance of *hgcA* was found in these paddy soil samples. This study not only systematically explored the influence of temperature and microsystem on CRISPR/Cas12a, providing vital references for other novel CRISPR-based detection methods, but also applied the CRISPR-based analytical method to the field of environmental geochemistry for the first time, demonstrating enormous potential for POU detection in this field.

* Corresponding authors.
E-mail addresses: maokang@mail.gyig.ac.cn (K. Mao), zhanghua@mail.gyig.ac.cn (H. Zhang).

https://doi.org/10.1016/j.scitotenv.2023.168536
Received 9 August 2023; Received in revised form 21 October 2023; Accepted 10 November 2023
Available online 17 November 2023

Environmental implication

This study reports a POU analysis for *hgcA* using a coupling gRNA-based CRISPR/Cas12a biosensor in a thermally stable microsystem that demonstrates low background, high sensitivity and specificity over a wide temperature range, providing a promising tool for on-site detection of the *hgcA* gene in paddy soil for evaluating MeHg exposure.

1. Introduction

Mercury (Hg) is the only global pollutant among all heavy metals that has been addressed at international conventions, to date, the Minamata Convention (Meng et al., 2021; Shao et al., 2016; Wu et al., 2016). The toxicity of different forms of mercury varies greatly, and methylmercury (MeHg) in particular is highly toxic (Braaten et al., 2019; Selin, 2009; Wu et al., 2020; Zhang et al., 2010; Zhang et al., 2022). Previous studies found that rice can accumulate MeHg with much higher efficiency than other crops and has become the main exposure source in some areas (Chang et al., 2020; Hsu-Kim et al., 2018; Zhang et al., 2010). Herein, to achieve the safe use of farmland and ensure food security, it is urgent to evaluate the MeHg risk in paddy soil, especially in paddy soil systems with serious mercury pollution, such as those near abandoned mercury mining areas (Feng et al., 2022).

Studies have found that MeHg in rice is absorbed from paddy soil by roots and that the main source of MeHg in paddy soil is microbially mediated mercury methylation (Capo et al., 2022; Regnell and Watras, 2019; Wang et al., 2014; Zhao et al., 2020). Utilizing the corrinoid protein encoded by the *hgcA* gene as a methyl donor to transfer methyl group from CH_3-H_4 folate to cob(*I*)alamin-*HgcA,* which can be further reduced to MeHg, is a key step in microbial mercury methylation in paddy soil (Fleming Emily et al., 2006; Ma et al., 2019; Parks Jerry et al., 2013; Wu et al., 2020). Therefore, soil *hgcA* could be used as a biomarker to indicate the potential capacity of microbial mercury methylation and further reflect the potential risk of MeHg. For example, Liu et al. found that the abundance of *hgcA* was positively correlated with the concentration of MeHg in soil (Liu et al., 2014).

Currently, the main methods of analysing *hgcA* are metagenomic sequencing and qPCR (Christensen et al., 2019; Liu et al., 2018). Although the former can provide detailed sequence information and the latter can generate quantitative data with high sensitivity and specificity, the tedious pretreatment process, expensive analysis and reliance on complicated equipment and professionals restrict their utilization on site (Kugelman et al., 2015; Zhao et al., 2015). Due to the limitations of analytical methods, *hgcA* cannot yet be applied to on-site rapid screening of the potential risk of MeHg. Therefore, developing a point-of-use (POU) method that can detect *hgcA* on site at a large scale is of great significance.

Clustered Regularly Interspaced Short Palindromic Repeats (CRISPR) is a milestone biotechnology, and CRISPR/Cas12a is a representative method (Chen Janice et al., 2018; Knott Gavin and Doudna Jennifer, 2018). Under the guidance of only one gRNA, Cas12a can recognize target DNA with high precision, and its trans-cleavage is then activated to cleave ssDNA probes nonspecifically (Chen Janice et al., 2018). Due to its high ssDNA cleavage efficiency and great compatibility with various modification groups, Cas12a can be used to construct different signal transductions, such as fluorescence, lateral flow analysis and colorimetry, depending on different conditions (English Max et al., 2019; Gootenberg Jonathan et al., 2018). Additionally, the method is easy to operate and can be conducted at constant temperature (Wang et al., 2022). Moreover, although no systematic studies have been performed, the Cas12a-gRNA complex might have a wide active temperature range (Ooi et al., 2021). Due to its high specificity (which could even reach to few bases), efficient signal transduction and extraordinary signal amplification capability as well as no need for thermal cycle etc., CRISPR/Cas12a-based biosensors are promising for POU detection (de Puig et al., n.d.; Kang et al., 2022; Luo et al., 2022).

Although CRISPR/Cas12a has exhibited great advantages, issues such as background signal interference and insufficient sensitivity limit its further application. The Cas12a-gRNA complex still exhibits trans-cleavage activity to some extent even without a target, which generates a background signal (Wang et al., 2020). Considering that POU detection usually does not involve high-resolution equipment, background signals may seriously interfere with the results. In addition, the reagent cost of CRISPR/Cas12a restricts its wide application. Moreover, the sensitivity of CRISPR/Cas12a is not sufficient for low-concentration samples without auxiliary signal magnification models, such as pre-amplification. For example, Chen and Tang et al. found that it was difficult to directly detect samples with concentrations lower than 10 pM using CRISPR/Cas12a (Chen Janice et al., 2018; Tang et al., 2022). Although some studies have tried to combine isothermal amplification with CRISPR/Cas12a to improve the sensitivity and obtained ideal results, the process increased the operation complexity, especially when the reaction conditions, such as LAMP preamplification and Cas12a cleavage, were different (Chen Janice et al., 2018; Feng et al., 2021). Therefore, it is very important to optimize the detection system to overcome the interference of background signals, improve the sensitivity, and simultaneously decrease the analysis cost without preamplification.

Above all, a thermal stable microsystem based CRISPR/Cas12a biosensor with coupling gRNA assay was developed in this study to achieve low-cost, highly sensitive and specific detection of *hgcA*. First, the Cas12a protein enAsCas12a-HF1 was selected due to its high activity and wide PAM (protospacer adjacent motif) compatibility, and then three gRNAs that specifically target *hgcA* were designed and validated. Next, we optimized the detection method by developing a microsystem to significantly reduce the strong background signal. Then, systemic research on the effect of temperature on the activity of the Cas12a-gRNA complex was conducted to explore its thermal stability. Additionally, a coupling gRNA assay was introduced to improve the sensitivity. The method was finally applied to *hgcA* detection in paddy soil to explore its relationship with Hg and MeHg and provide information for MeHg risk assessment. We hope the newly developed POU method consumes an extremely low amount of reagents and exhibits a faster reaction rate, higher sensitivity and negligible background signal compared to that of the traditional CRISPR/Cas12a analytical platform, providing a potential POU tool for on-site screening of *hgcA* in paddy soil at a large scale.

2. Materials and methods

2.1. Materials and reagents

NEB Buffer 2.1 (B7202S) was purchased from New England Biolabs (USA), gRNAs were synthesized by Bio-Lifesci (China), plasmid pUC-GW-Kan containing *hgcA* was constructed by Genewiz (USA), and the sequences are shown in Table S1. Competent DH5α (B528413–0010), lsopropyl-beta-D-thiogalactopyranoside (IPTG, A100487), tris(2-carboxyethyl) phosphine (TCEP, A600974) and ssDNA probes were obtained from Sangon Biotech (China). UltraPure™ DNase/RNase-Free Distilled Water (10977023) was purchased from Thermo Fisher Scientific (USA). The plasmid for the expression of enAsCas12a was from Miaoling Biotechnology Co., Ltd. (China). Kanamycin (K8020) was purchased from Solarbio LIFE Sciences (China), cocktail protease inhibitor (S25910) and 1 M HEPES (R20072) were purchased from Yuanye Bio-Technology Co., Ltd. (China).

2.2. Preparation of enAsCas12a-HF1

The plasmid pET-28b-T7-henAsCas12a-HF1 was first transfected into competent Rosetta 2(DE3) cells by heat shock treatment followed by inoculation into broth agar medium containing 50 mg/L kanamycin and 30 mg/L chloramphenicol. After growing overnight at 37 °C, the successfully transformed strain was selected and then inoculated into

100 mL of dual-resistant liquid broth medium. After growing to saturation at 37 °C and 220 RPM, 20 mL of saturated bacterial solution was transferred to 1 L of dual-resistant liquid broth medium and cultured to logarithmic metaphase. Then, IPTG was added to the solution to induce expression with a final concentration of 0.1 mM. The bacteria were then collected by centrifugation at 4 °C and 5000 xg for 10 min after expression at 18 °C for 18 h. Finally, the bacteria were stored at −80 °C until purification.

The bacteria were thawed on ice followed by lysis with lysis buffer (20 mM HEPES pH 7.5, 300 mM NaCl, 2 mM $MgCl_2$, 20 mM imidazole, 0.5 mM TCEP, 0.1 % Triton X-100, 0.25 mg/mL lysozyme, 1:100 protease inhibitor) and ultrasound. The ratio of bacteria to lysis buffer was 1:5. Then, the lysate was centrifuged at 40000 xg for 1 h 30 min at 4 °C to separate the proteins and bacteria. After that, the supernatant was loaded into a Histrap HP (Cytiva, USA) and eluted linearly with buffer A (50 mM Tris HCl, pH = 8.0, 20 mM imidazole, 300 mM NaCl, 0.5 mM TCEP) and buffer B (50 mM Tris HCl, pH = 8.0, 300 mM imidazole, 300 mM NaCl, 0.5 mM TCEP) at Akta pure 25 M (Cytiva, USA). The buffer was then exchanged to Buffer C (20 mM Tris-HCl, pH 7.5, 200 mM NaCl, 10 % (*v*/v) glycerol) by a desalting column. Finally, the protein was concentrated to 10 μM by ultrafiltration, and its concentration was determined by a Qubit 4.0 fluorometer. The purified protein was stored at −80 °C until use.

2.3. Preparation of the hgcA-containing plasmid

After the construction of the plasmid, it was transfected into competent DH5α cells by heat shock treatment. Then, the bacteria were inoculated into LB agar medium containing 50 mg/L kanamycin. An adequate colony was selected after overnight growth at 37 °C and then inoculated into 100 mL kanamycin-resistant liquid LB medium. After growing to saturation, the plasmid was extracted by a Tiangen plasmid small extraction kit (DP103) according to the manufacturer's instructions. The concentration was analysed by a Qubit 4.0 fluorometer. Finally, the plasmid was stored at −80 °C until use.

2.4. Construction of the initial CRISPR/Cas12a system

The preassembling solution containing 1 μM Cas12a, 1.25 μM gRNA and 1 X NEB buffer 2.1 was first incubated at 37 °C for 10 min. Then, 2 μL of the complex was transferred to 16 μL of 1 X NEB buffer 2.1 solution containing plasmids of different concentrations and 2 μL of 5 μM ssDNA probes. Next, the reactions were incubated at 37 °C for 60 min, and the fluorescence was collected by qPCR (ABI7500). Four parallel reactions were performed for each concentration.

2.5. Construction of the microsystem

The preassembly procedure was similar to the construction of the initial CRISPR/Cas12a system. Then, the solution was diluted 10, 100, and 1000 times, and 2 μL aliquots of diluted complexes with different contents were added to 16 μL of 1 X NEB buffer 2.1 solution containing 1.25 nM *hgcA* and 2 μL of 5 μM ssDNA probes. The solution was then incubated at 37 °C for 60 min, and the fluorescence was collected by qPCR (ABI7500) each minute. Four parallel reactions were performed.

2.6. Evaluation of thermal stability

The preassembly method was similar to the construction of the initial CRISPR/Cas12a system. After that, the liquid was diluted 100 times. Then, 2 μL diluted complex was transferred to 16 μL solution containing 1.25 nM *hgcA* in 1 × NEB buffer 2.1. The precleavage liquid was incubated at 37 °C for 20 min. Finally, 2 μL aliquots of ssDNA probes of different concentrations were added to the system. The final concentrations of the probes were 15.63, 31.25, 62.5, 125, 250, 500, and 1000 nM. Then, the reactions were incubated at 25, 32, 37, 42, 47, 52, 57, and 62 °C for 60 min, respectively.

2.7. Development of the coupling gRNA-based CRISPR/Cas12a detection method

After complex assembly was performed according to construction of the initial CRISPR/Cas12a system, Cas12a-gRNA1–2 was diluted 3.3 times, while Cas12a-gRNA3 was diluted 33.3 times. Then, 0.67 μL of each complex was added to 18 μL solutions containing ssDNA probes and different concentrations of *hgcA* in 1 × NEB buffer 2.1. The final probe concentration was 500 nM. Finally, the reaction was incubated at 47 °C for 1 h, and the fluorescence was recorded.

2.8. Sample collection and hgcA detection

The soil samples were collected from paddy soil system at a depth of 0–20 cm with five-point sampling method in Sikeng of Tongren (109°12′11″E, 27°30′38″N) and Leizhuang of Guiyang (106°31′41″E, 26°23′26″N) of Guizhou Province, China, in August and October 2022. The former was polluted by mercury mining activity and was selected as a representative polluted site, while the latter was free of anthropogenic activities and was selected as a low-mercury site. After removing impurities, such as rice roots and stones, the DNA in the soil samples was extracted via a commercial kit according to the instructions (Qiagen Powersoil Kit). Then, the samples were analysed by a coupling gRNA-based CRISPR/Cas12a biosensor with a thermal stable microsystem. For the spiked test, different concentrations of plasmids containing *hgcA* were added to soil DNA samples without *hgcA* before determination. The fluorescence was also recorded by qPCR (ABI7500), while for visualization detection, solutions after incubation were excited by a 480 nm illuminant, and the grey data were extracted by ImageJ.

3. Results and discussion

3.1. Sensing principle and feasibility exploration

The sensing principle is shown in Scheme 1. In the presence of *hgcA*, Cas12a could recognize and cleave the target fragment specifically under the guidance of gRNA. Then, the trans-cleavage activity was activated, and ssDNA probes were cleaved rapidly and nonspecifically. Carboxyfluorescein (FAM) and Black Hole Quencher-1 (BHQ-1), which had been linked by ssDNA, were separated. Then, the quenched fluorescence was recovered and could be observed. However, in the absence of target, Cas12a-gRNA could not be activated, and the probes remained intact. FAM and BHQ-1 remained linked, and the fluorescence could not be recovered. Thus, no fluorescence could be observed.

Next, three gRNAs were initially designed to specifically target *hgcA*, followed by the construction of three amplification-free CRISPR/Cas12a detection platforms according to previous methods (Lin et al., 2022; Ma et al., 2022). Different concentrations of plasmids containing *hgcA* were further utilized to assess the analytical performance. As shown in Fig. S1, the endpoint fluorescence was significantly higher than the background when the target concentration was 500 pM for the three CRISPR/Cas12a systems, indicating that *hgcA* was successfully detected. Similar results were also obtained from the real-time fluorescence curves of these assays (Fig. S1).

Although the methods could detect *hgcA*, their performance was not satisfactory. As demonstrated in Fig. S1, the background signal of Cas12a-gRNA1 reached 5.8×10^5 AU, while its limit of detection (LOD) was only 250 pM. The subtracted fluorescence was only approximately 1.5×10^5 AU, even for samples with 500 pM *hgcA*. Therefore, the fluorescence generated by the activated Cas12a-gRNA1 complex was easily interfered by the background signal, especially for samples with lower concentrations. Based on the results, we speculated that the LOD of Cas12a-gRNA1 may be lower than 250 pM, but the detection signal at lower concentrations was annihilated by the overly strong background

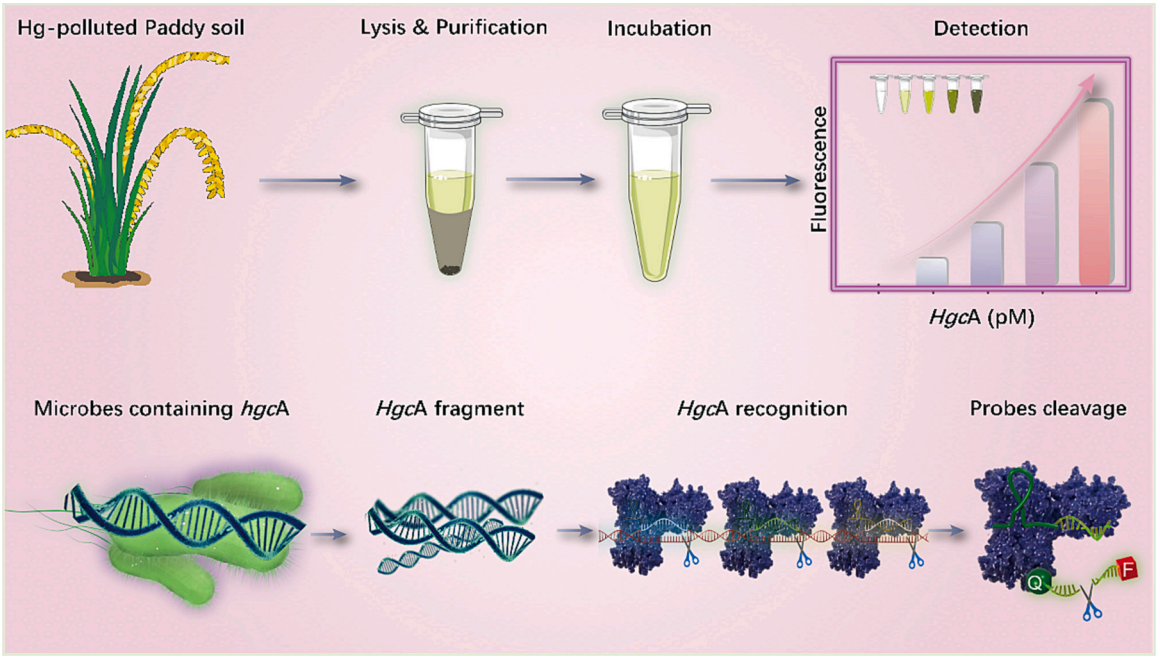

Scheme 1. Mechanism of detecting *hgcA* using the CRISPR-based biosensor in paddy soil. Upper part: Process of detecting *hgcA* in paddy soil. The paddy soil was first collected, followed by microbe lysis and DNA purification to prepare the samples. Then, the purified DNA was added to the CRISPR/Cas12a detection system. After the samples were incubated, the results could be obtained by a fluorescence reader or visualized by blue light. Lower part: Molecular mechanism of detecting *hgcA* in paddy soil. Microbes released nucleic acids through lysis, and three Cas12a-gRNA complexes then recognized target *hgcA* fragments via base pairing followed by specifically cleaving the target. Next, the trans-cleavage activity was activated, and ssDNA probes were cleaved rapidly. Finally, FAM and BHQ-1 were separated, and fluorescence occurred.

signal.

Cas12a-gRNA2 and 3 exhibited lower background signals than Cas12a-gRNA1, but the signals still reached 1.0–2.0 × 10^5 AU (Fig. S1). The LODs of Cas12a-gRNA 2 and Cas12a-gRNA 3 were also lower than that of Cas12a-gRNA1 and reached 62.5 pM. Considering that the background signal may also seriously interfere with the reactions, their actual LODs may also be significantly lower than 62.5 pM.

Above all, if the background signal could be thoroughly reduced to prevent interference, the sensitivity of this method might be greatly improved. Therefore, the reactions were next optimized to reduce the

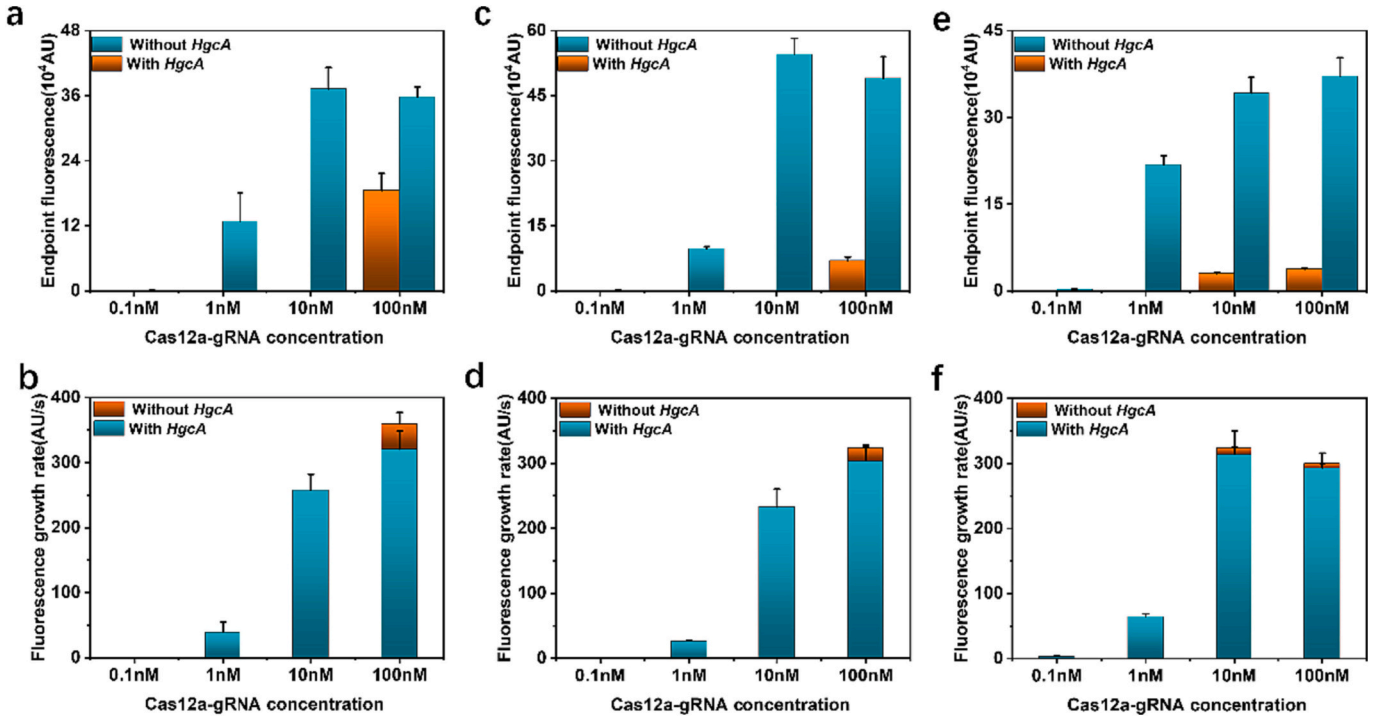

Fig. 1. Detection performance of different concentrations of Cas12a-gRNA. a-c: Endpoint fluorescence of detecting blank samples and 1 nM *hgcA* with different concentrations of Cas12a-gRNA1–3. d-f: Fluorescence growth rate of detecting 1 nM *hgcA* and blank samples with different concentrations of Cas12a-gRNA1–3.

background signal.

3.2. Microsystem optimization

The concentration of the Cas12a-gRNA complexes in the study was 100 nM, which was similar to that used in previous studies (Lin et al., 2022; Ma et al., 2022). However, the target concentrations were much lower than those of the complexes, indicating that the complexes were largely in excess, which may lead to a strong background signal. An experiment with complex concentration as the only variable was then conducted to verify this speculation. As shown in Fig. 1 and Fig. S2, the background signal was reduced to 0 for Cas12a-gRNA1 and Cas12a-gRNA2 when the concentration was decreased from 100 nM to 10 nM, suggesting that background cleavage was completely suppressed. Interestingly, the endpoint signal and reaction velocity of the experimental group with *hgcA* did not decrease significantly. However, when the complex concentration further decreased to 1.0 nM, both the endpoint and reaction velocity decreased dramatically. Moreover, the reaction was nearly stopped when the content of the complex was reduced to 0.1 nM. Therefore, 10 nM was more suitable for Cas12a-gRNA1, 2, and due to the low reagent usage, we named the chosen conditions the microsystem.

Notably, since the target content was 1.0 nM, Cas12a-gRNA1 and Cas12a-gRNA2 were all saturated or in excess when they were reduced from 100 nM to 1.0 nM, and the concentration of the activated complex did not change. Therefore, the changes in endpoint fluorescence and reaction velocity were mainly caused by the differences in the complex activities. The complex activities did not change significantly when the complexes were reduced from 100 to 10 times the target concentration, but the activities decreased sharply when the complexes were further reduced; thus, an appropriate excess amount of Cas12a-gRNA could greatly improve their trans-cleavage. However, a large amount of excess complex did not further improve the reaction activity and caused high background signals. Thus, it was critical to select an appropriate complex concentration when constructing the CRISPR/Cas12a biosensor.

The change in Cas12a-gRNA3 was similar to that of Cas12a-gRNA1, 2, while its content needed to be reduced to 1.0 nM to thoroughly reduce the background signal. Although the reaction rate was greatly decreased at this time, considering that the intensity of its end-point fluorescence signal remained strong enough for detection, sacrificing the reaction rate in exchange for eliminating the background signal was undoubtedly worthwhile. Therefore, 1.0 nM was more suitable for Cas12a-gRNA3 utilization in the reaction. The different suitable amounts between Cas12a-gRNA1, Cas12a-gRNA2 and Cas12a-gRNA3 also indicated that the optimal concentration was not always similar for different gRNAs. It was very important to explore the optimal concentration of Cas12a-gRNA to develop the CRISPR/Cas12a-based analytical platform. However, concentration optimization has always been omitted in the construction of CRISPR/Cas12a detection systems.

3.3. Thermal stability exploration of Cas12a-gRNA

Considering that precision instruments are generally lacking in on-site conditions, the strict temperature requirements of previous CRISPR/Cas12a detection methods restrict their further application for POU detection. Fortunately, a recent study showed that a variant of enAsCas12a-HF1 exhibited strong activity over a wide temperature range (Ooi et al., 2021). Therefore, enAsCas12a-HF1 may possess similar characteristics, indicating that accurately controlling the temperature may not be necessary for detection. Based on this speculation, the first systematic study on the effect of temperature on Cas12a-gRNA activity was carried out in this work. The kinetic characteristics of Cas12a-gRNA trans-cleavage activity were tested from 25 °C to 62 °C. As demonstrated in Fig. S3, the endpoint fluorescence was much higher at 37–57 °C, while it decreased sharply when the temperature was reduced to 32 °C or increased to 62 °C. The results indicated that the appropriate temperature range for the reaction was 37 °C to 57 °C, which was different from that found in Benjamin P. Kleinstiver's research, although the two enzymes were almost the same except for amino acids at the 282nd site (Kleinstiver et al., 2019). A detailed experiment was then conducted to explore the reaction kinetics between 37 °C and 57 °C. Then, to prevent the interference of fluorescence fluctuation in the analysis and better explore kinetic parameters such as Km and Kcat, the fluorescence was also converted to the amount of substrate cleavage (Figs. S4-S9).

As shown in Fig. 2a-c, the Km of Cas12a-gRNA 1–3 exhibited a similar trend between 37 °C and 57 °C. With increasing temperature, the values first increased, then decreased and then increased again. Small Km values were all obtained at 47 °C, indicating that the affinity was high under these conditions. The Km increased sharply when the temperature increased from 52 °C to 57 °C, suggesting that the affinity between the complex and substrate decreased dramatically when the temperature exceeded 52 °C. For Kcat, Cas12a-gRNA1 exhibits a different tendency from its Km, which decreased slightly from 37 °C to 42 °C and continuously increased when the temperature increased from 42 °C to 57 °C. For Cas12a-gRNA2 and 3, the change trend of Kcat was the same as that of Km, and small values were obtained at 37 °C and 47 °C, suggesting that the catalytic efficiency was lower than that under other conditions. Notably, the Kcat of all three complexes increased significantly when the temperature rose from 52 °C to 57 °C and reached the highest value at 57 °C, even exceeding 10 times that at 37 °C. This phenomenon indicated that the catalytic efficiency increased sharply when the temperature exceeded 52 °C. Overall, the complex exhibited high substrate affinity at low temperature and high catalytic efficiency at high temperature.

Considering the effect of temperature on affinity and catalytic efficiency, Kcat/Km was then utilized to comprehensively evaluate the effect. The three complexes demonstrated similar tendencies, which first increased and then failed with increasing temperature. The Kcat/Km of Cas12a-gRNA2 and Cas12a-gRNA3 both reached their highest values at 47 °C and exhibited high values at 42–57 °C and 37–57 °C, respectively. For the Kcat/Km of Cas12a-gRNA1, the highest value was obtained at 52 °C, and high values were obtained between 47 and 52 °C. The different thermal features between Cas12a-cgRNA1 and Cas12a-gRNA2 and 3 might be caused by different energies of hybridization between the target sequences and gRNAs, which could affect the stability and characteristics of the cleavage conformation of the complexes (Zhang et al., 2019). Above all, the thermal stability of the complex was successfully verified in the experiment, while they had a suitable reaction temperature range as wide as 20 °C and a better reaction temperature range of 5–20 °C. Therefore, accurately controlling the temperature is not necessary when using this assay for detection, which further reduces the requirements for field conditions. Moreover, different from the traditional insight, 47 °C might be more suitable for the reaction than 37 °C (Hang et al., 2022). The Kcat/Km of Cas12a-gRNA1–3 was 2.85, 2.37 and 1.64 times higher than that at 37 °C, respectively, indicating that increasing the temperature from 37 °C to 47 °C significantly improved the trans-cleavage activities of the complexes. Therefore, 47 °C was selected as the optimal temperature to better evaluate the analytical performance.

3.4. Coupling gRNA to improve sensitivity

After the above reaction optimization, the linear ranges and LODs of Cas12a-gRNA1–3 were tested. As shown in Fig. 3a-f and S10 a-c, their linear ranges were 3.9–125 pM, 1.95–125 pM and 15.63–125 pM, respectively. Their LODs reached 3.9 pM, 1.95 pM and 15.63 pM, respectively, which were 64 times, 32 times and 4 times lower than those of the nonoptimized method. Considering that *hgcA* may not be highly abundant in paddy soil, further improving the sensitivity and lowering the LOD are needed.

Recent studies have shown that using multiple gRNAs in CRISPR/

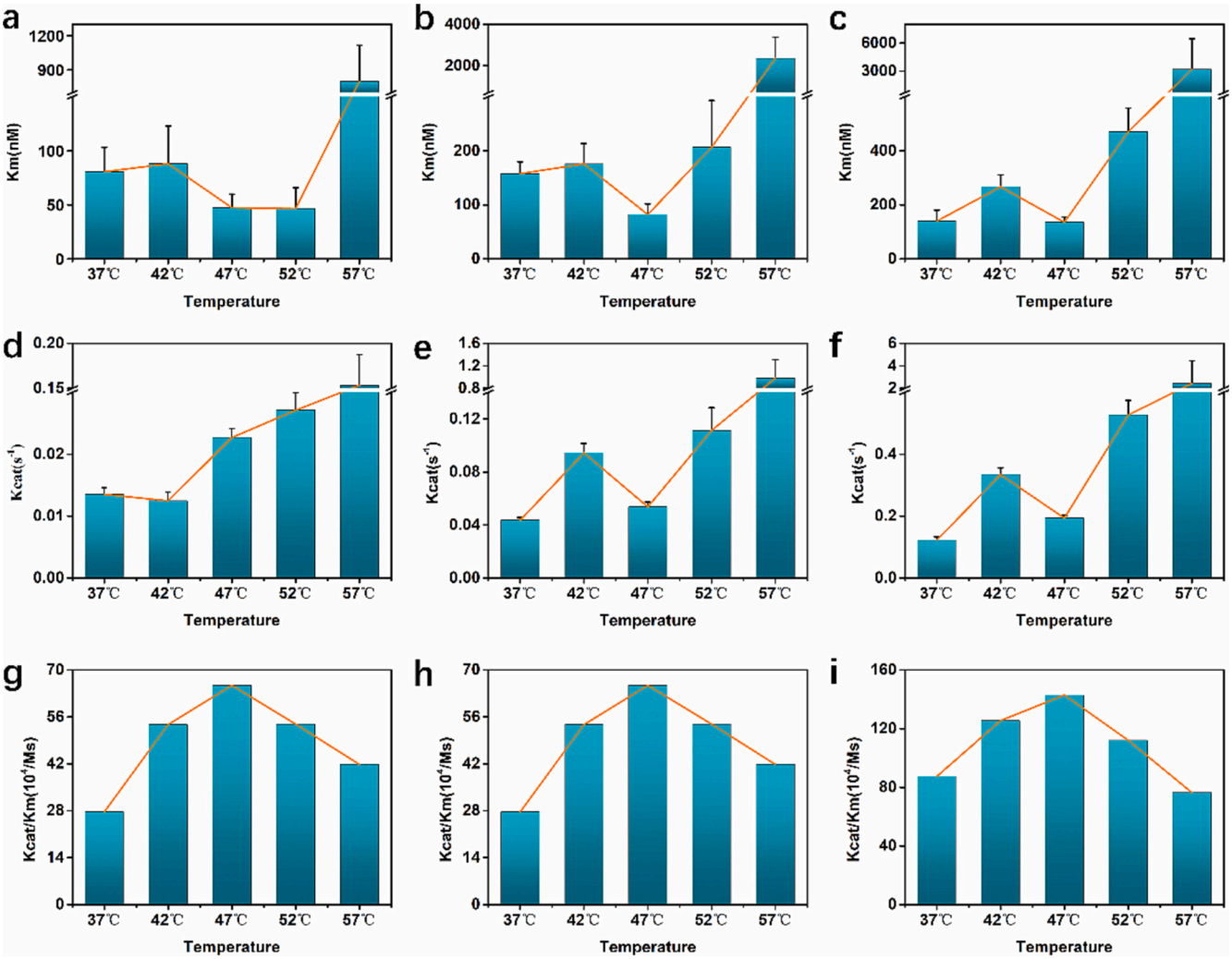

Fig. 2. Variation in Km, Kcat and Kcat/Km of Cas12a-gRNA from 37 °C to 57 °C. a-c: Km variation of Cas12a-gRNA1–3 from 37 °C to 57 °C. d-f: Kcat variation of Cas12a-gRNA1–3 from 37 °C to 57 °C. g-i: Cas12a-gRNA1–3 Kcat/Km variation of Cas12a-gRNA1–3 from 37 °C to 57 °C. For the measurement of Kcat and Km, the reaction curves of 1 nM activated Cas12a-gRNA at substrate concentrations from 15.63 to 1000 nM were measured to obtain their initial reaction velocities. Then, the scatter plots of the velocities and substrate concentrations were drawn, followed by nonlinear fitting with the Michaelis–Menten curve. Finally, Kcat and Km could be directly obtained from the parameters of the Michaelis–Menten curve in Origin software.

Cas12a analysis could improve its sensitivity (Zeng et al., 2022). Therefore, the technology was introduced to construct a coupling gRNA-based CRISPR/Cas12a biosensor with a thermal stable microsystem. In general, the coupling gRNA system was constructed by mixing three gRNAs with the optimal concentrations obtained above, while the other conditions did not change. As shown in Fig. 3 g-h, the method could detect *hgcA* as low as 0.49 pM, which was four times lower than the most sensitive single-gRNA assay. The linear range of the assay was 0.98–125 pM, which was more than three orders of magnitude. Moreover, the signal in the coupling gRNA method was also significantly higher than the sum of three single gRNA assays, and its background signal remained zero. These results demonstrated that the coupling system was not a simple superposition of the three systems and that a synergistic effect appeared. First, due to the low sensitivity of Cas12a-gRNA1 and Cas12a-gRNA3 compared to Cas12a-gRNA2, the LOD of the coupling method should be approximately 1.95 pM if it is a simple superposition. Second, the fluorescence signal of the coupling platform should be similar to the sum of three single gRNA assays if no synergistic effects occur. However, the coupling system not only had a much lower LOD but also possessed much stronger fluorescence. Due to similar reaction conditions between coupling gRNA and single gRNA, the reason for the results might be that different complexes could enhance the reactivity and sensitivity of each other, and synergistic trans-cleavage appeared (Zeng et al., 2022).

Then, we explored whether synergistic effects occurred in the coupling of any two gRNAs. As shown in Fig. S11, the detection limits for gRNA1 + 2, gRNA1 + 3 and gRNA2 + 3 were 3.9, 7.8 and 7.8 pM, respectively, which were even higher than the LOD of the most sensitive gRNA in the combination system. The results suggested that the coupled gRNA could not always lower the LOD and might even decrease the sensitivity in some conditions, such as crRNA1 + 2 and crRNA1 + 3. Both synergistic and antagonistic effects might exist in the coupling system. We speculate whether synergistic or antagonism effect present depending on the sequences of coupling gRNAs to a great extent. Further studies are needed to explore the changes in complex features in the coupling system to clarify the molecular mechanism of synergistic or antagonistic effects, which might be critical for the popularization of the method.

After the sensitivity evaluation, a specificity test was carried out to assess the anti-interference ability of the method, which is critically important in POU detection. Three additional mercury metabolism-related genes (*hgcB, merA* and *merB*) and two additional methylation-related genes, *arsM* (As methylated gene) and *tpm* (Se methylated gene), were selected as interference genes. As shown in Fig. S12, the signal could only be observed in the presence of *hgcA,* while there was

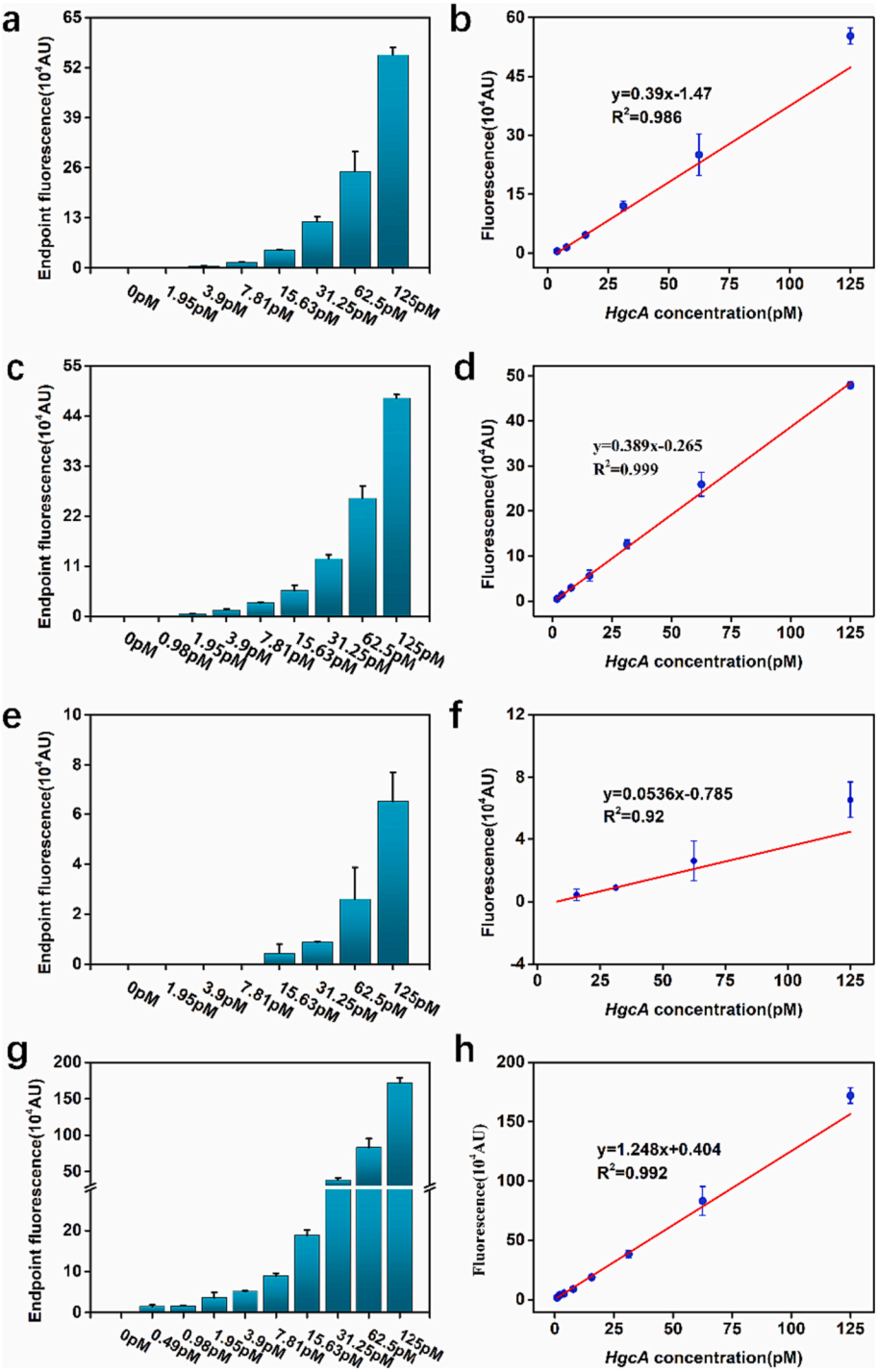

Fig. 3. Evaluation of LOD and linear fitting between endpoint fluorescence and *hgcA* concentration. a, c, e, g: Endpoint fluorescence of optimized Cas12a-gRNA1, 2, 3 and the constructed detection method. b, d, f, h: Linear fitting between endpoint fluorescence and *hgcA* concentration of optimized Cas12a-gRNA1, 2, 3 and the constructed detection method.

almost no signal even when the concentration of the interference genes reached 1 nM, indicating that the method had satisfactory specificity.

Above all, the system developed here demonstrated high sensitivity, a wide linear range and a fast reaction speed, which allowed completion in one hour, especially compared with amplification-free CRISPR detection methods for other targets, such as pathogens and microRNA, while the sensitivities were often near the pM level to the nM level (Table S2). In particular, it is worth mentioning that the LOD was even lower than that of some previous methods developed by a combination of isothermal amplification and CRISPR technology (Table S2).

3.5. Validation of analytical methods in paddy soil samples

Considering that the recognition region of Cas12a is only approximately 20 bases and that there are many microorganisms in paddy soil, it was unclear whether the novel analytical method would be affected by other nucleic acids in soil. Therefore, plasmids containing *hgcA* were spiked into soil samples without *hgcA* to evaluate the biosensor's performance with actual samples.

As shown in Fig. 4a-b, there were no signals in the samples without *hgcA*, indicating that the assay could completely resist the interference

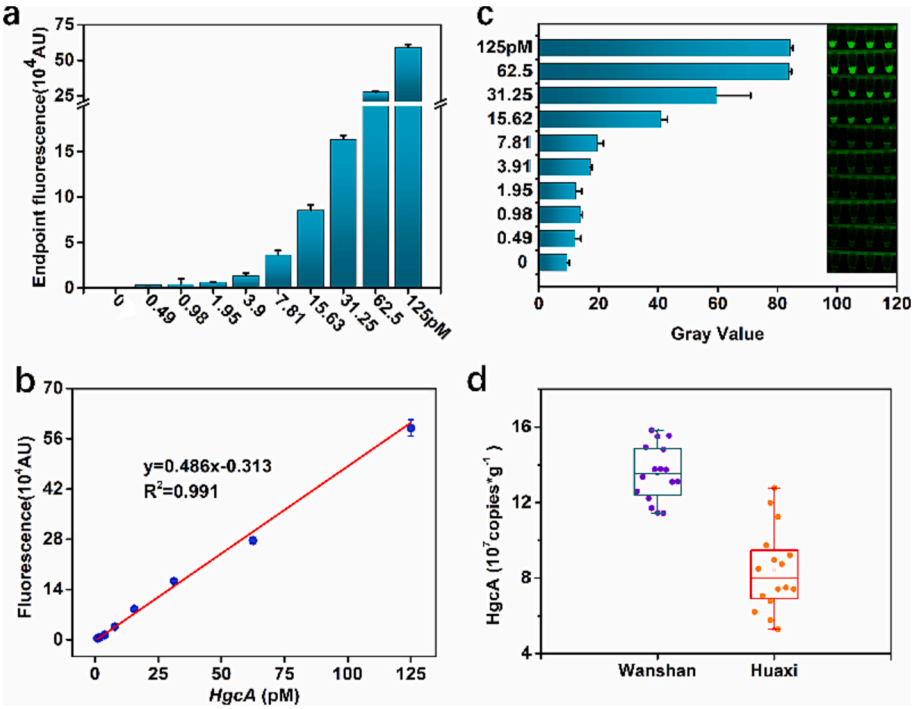

Fig. 4. Detection performance of coupling gRNA-based CRISPR/Cas12a biosensor with a thermal stable microsystem detection method for paddy soil samples. a: Endpoint fluorescence of samples spiked with different contents of *hgcA*. b: Linear fitting of endpoint fluorescence and *hgcA* contents. c: Visualization results of different contents of *hgcA* and their grey values extracted by ImageJ. d: Detection results of *hgcA* abundance in paddy soil of Tongren and Guiyang.

of various microbial genomes and plasmids in soil even when their concentration exceeded 10^4 μg/g (DNA contents in paddy soil utilized in this study were (1.1–1.6) × 10^4 μg/g). Moreover, the sensitivity and quantitative ability of the method were not influenced, the LOD remained as low as 0.49 pM, and the linear range was 0.98 pM-125 pM. Additionally, the recovery rate of the platform was 90–110 %, indicating its excellent quantitative capability (Table S3).

Considering that no fluorescence equipment may be present on site, a visual method was further developed. After incubation, the results could be observed by the naked eye under the excitation of a 480 nm portable illuminant. As shown in Fig. 4c, the sensitivity of the visual assay also reached 0.49 pM and was identical to that obtained from a thermal cycler (ABI7500). Moreover, the visual results could be further processed by ImageJ to achieve semiquantitative analysis, which could provide more information for the screening of *hgcA* and on-site assessment of potential MeHg risks.

Finally, we applied the method for on-site screening of *hgcA* in the Tongren Hg Mine area of China, while Guiyang was chosen as a low-mercury area for comparison. As shown in Fig. 4d and Table S4, the abundances of *hgcA* in Wanshan and Huaxi were 13.55 ± 1.46 × 10^7 copies/g and 8.41 ± 2.18 × 10^7 copies/g, respectively, and detailed information is shown in Table S4. The higher abundance of *hgcA* in the mining area further demonstrated that *hgcA* could be used to indicate mercury pollution and that its POU detection might be useful for the rapid screening of mercury risk areas.

4. Conclusions

In this study, for the first time, an amplification-free CRISPR/Cas12a-based sensitive biosensor with a thermal stable microsystem was developed to detect the *hgcA* gene, a critical biomarker of MeHg in paddy soil. When constructing the detection system, we thoroughly optimized the existing CRISPR/Cas12a system, including significantly improving the detection performance by introducing microsystem, further reducing the requirements for site conditions by finding its thermal stability, coupling gRNA to further improve sensitivity, etc. This optimized method exhibited a wide linear range with high selectivity and sensitivity and could be completed within 1.0 h. Moreover, validation with real paddy soil samples demonstrated that the method had excellent anti-interference ability in complicated samples. Therefore, the method holds great potential for POU detection and is expected to provide critical support for rapidly screening MeHg risk in paddy soil through *hgcA*.

CRediT authorship contribution statement

Haorui Cao: Investigation, Methodology, Writing – original draft, Writing – review & editing. **Kang Mao:** Investigation, Methodology, Writing – original draft, Writing – review & editing. **Hua Zhang:** Investigation, Supervision. **Qingqing Wu:** Investigation. **Huangxian Ju:** Writing – review & editing. **Xinbin Feng:** Supervision.

Declaration of competing interest

The authors declare that they have no known competing financial interests or personal relationships that could have appeared to influence the work reported in this paper.

Data availability

The data that has been used is confidential.

Acknowledgements

The authors acknowledge support from the National Natural Science Foundation of China (42107486, 42377456), Guizhou Provincial Science and Technology Projects (Qiankehe Jichu-ZK [2022] Yiban 565), Guizhou Provincial 2021 Science and Technology Subsidies (No. GZ2021SIG), Youth Cross Team Project of CAS (JCTD-2021-17), and the Youth Innovation Promotion Association CAS (2023415).

Appendix A. Supplementary data

Supplementary data to this article can be found online at https://doi.org/10.1016/j.scitotenv.2023.168536.

References

Braaten, H.F.V., Åkerblom, S., Kahilainen, K.K., Rask, M., Vuorenmaa, J., Mannio, J., Malinen, T., Lydersen, E., Poste, A.E., Amundsen, P.-A., et al., 2019. Improved environmental status: 50 years of declining fish mercury levels in boreal and subarctic fennoscandia. Environ. Sci. Technol. 53 (4), 1834–1843. https://doi.org/10.1021/acs.est.8b06399.

Capo, E., Feng, C., Bravo, A.G., Bertilsson, S., Soerensen, A.L., Pinhassi, J., Buck, M., Karlsson, C., Hawkes, J., Björn, E., 2022. Expression levels of hgcAB genes and mercury availability jointly explain methylmercury formation in stratified brackish waters. Environ. Sci. Technol. 56 (18), 13119–13130. https://doi.org/10.1021/acs.est.2c03784.

Chang, C., Chen, C., Yin, R., Shen, Y., Mao, K., Yang, Z., Feng, X., Zhang, H., 2020. Bioaccumulation of hg in Rice leaf facilitates selenium bioaccumulation in rice (Oryza sativa L.) leaf in the Wanshan mercury mine. Environ. Sci. Technol. 54 (6), 3228–3236.

Chen Janice, S., Ma, E., Harrington Lucas, B., Da Costa, M., Tian, X., Palefsky Joel, M., Doudna Jennifer, A., 2018. CRISPR-Cas12a target binding unleashes indiscriminate single-stranded DNase activity. Science 360 (6387), 436–439. https://doi.org/10.1126/science.aar6245.

Christensen, G.A., Gionfriddo, C.M., King, A.J., Moberly, J.G., Miller, C.L., Somenahally, A.C., Callister, S.J., Brewer, H., Podar, M., Brown, S.D., et al., 2019. Determining the reliability of measuring mercury cycling gene abundance with correlations with mercury and methylmercury concentrations. Environ. Sci. Technol. 53 (15), 8649–8663. https://www.ncbi.nlm.nih.gov/pubmed/31260289.

English Max, A., Soenksen Luis, R., Gayet Raphael, V., de Puig, H., Angenent-Mari Nicolaas, M., Mao Angelo, S., Nguyen Peter, Q., Collins James, J., 2019. Programmable CRISPR-responsive smart materials. Science 365 (6455), 780–785. https://doi.org/10.1126/science.aaw5122.

Feng, W., Peng, H., Xu, J., Liu, Y., Pabbaraju, K., Tipples, G., Joyce, M.A., Saffran, H.A., Tyrrell, D.L., Babiuk, S., et al., 2021. Integrating reverse transcription recombinase polymerase amplification with CRISPR technology for the one-tube assay of RNA. Anal. Chem. 93 (37), 12808–12816. https://doi.org/10.1021/acs.analchem.1c03456.

Feng, X., Li, P., Fu, X., Wang, X., Zhang, H., Lin, C.-J., 2022. Mercury pollution in China: implications on the implementation of the Minamata Convention. Environ. Sci. Processes Impacts 24 (5), 634–648. https://doi.org/10.1039/D2EM00039C.

Fleming Emily, J., Mack, E.E., Green Peter, G., Nelson Douglas, C., 2006. Mercury methylation from unexpected sources: molybdate-inhibited freshwater sediments and an iron-reducing bacterium. Appl. Environ. Microbiol. 72 (1), 457–464. https://doi.org/10.1128/AEM.72.1.457-464.2006.

Gootenberg Jonathan, S., Abudayyeh Omar, O., Kellner Max, J., Joung, J., Collins James, J., Zhang, F., 2018. Multiplexed and portable nucleic acid detection platform with Cas13, Cas12a, and Csm6. Science 360 (6387), 439–444. https://doi.org/10.1126/science.aaq0179.

Hang, X.-M., Zhao, K.-R., Wang, H.-Y., Liu, P.-F., Wang, L., 2022. Exonuclease III-assisted CRISPR/Cas12a electrochemiluminescence biosensor for sub-femtomolar mercury ions determination. Sens. Actuators B". 368, 132208. https://www.sciencedirect.com/science/article/pii/S0925400522008504.

Hsu-Kim, H., Eckley, C.S., Achá, D., Feng, X., Gilmour, C.C., Jonsson, S., Mitchell, C.P.J., 2018. Challenges and opportunities for managing aquatic mercury pollution in altered landscapes. AMBIO 47 (2), 141–169. https://doi.org/10.1007/s13280-017-1006-7.

Kang, Y., Su, G., Yu, Y., Cao, J., Wang, J., Yan, B., 2022. CRISPR-Cas12a-based Aptasensor for on-site and highly sensitive detection of microcystin-LR in freshwater. Environ. Sci. Technol. 56 (7), 4101–4110. https://doi.org/10.1021/acs.est.1c06733.

Kleinstiver, B.P., Sousa, A.A., Walton, R.T., Tak, Y.E., Hsu, J.Y., Clement, K., Welch, M. M., Horng, J.E., Malagon-Lopez, J., Scarfò, I., et al., 2019. Engineered CRISPR-Cas12a variants with increased activities and improved targeting ranges for gene, epigenetic and base editing. Nat. Biotechnol. 37 (3), 276 (://WOS:000460155900018).

Knott Gavin, J., Doudna Jennifer, A., 2018. CRISPR-Cas guides the future of genetic engineering. Science 361 (6405), 866–869. https://doi.org/10.1126/science.aat5011.

Kugelman, J.R., Wiley, M.R., Suzanne, M., Ladner, J.T., Brett, B., Lawrence, F., Fahn, T., Karla, P., Diclaro, J.W., Timothy, M.J.E.I.D., 2015. Monitoring of Ebola Virus Makona Evolution through Establishment of Advanced Genomic Capability in Liberia, 21 (7), pp. 1135–1143.

Lin, M., Yue, H., Tian, T., Xiong, E., Zhu, D., Jiang, Y., Zhou, X., 2022. Glycerol additive boosts 100-fold sensitivity enhancement for one-pot RPA-CRISPR/Cas12a assay. Anal. Chem. 94 (23), 8277–8284. https://doi.org/10.1021/acs.analchem.2c00616.

Liu, Y. R.; Yu, R. Q.; Zheng, Y. M.; He, J. Z. 2014. Analysis of the microbial community structure by monitoring an Hg methylation gene (hgcA) in paddy soils along an Hg gradient. Appl. Environ. Microbiol. 80 (9), 2874–2879. <Go to ISI>://WOS:000334583300027.

Liu, Y.R., Johs, A., Bi, L., Lu, X., Hu, H.W., Sun, D., He, J.Z., Gu, B., 2018. Unraveling microbial communities associated with methylmercury production in paddy soils. Environ. Sci. Technol. 52 (22), 13110–13118. https://www.ncbi.nlm.nih.gov/pubmed/30335986.

Luo, T., Li, J., He, Y., Liu, H., Deng, Z., Long, X., Wan, Q., Ding, J., Gong, Z., Yang, Y., et al., 2022. Designing a CRISPR/Cas12a- and Au-nanobeacon-based diagnostic biosensor enabling direct, rapid, and sensitive miRNA detection. Anal. Chem. 94 (17), 6566–6573. https://www.ncbi.nlm.nih.gov/pubmed/35451838.

Ma, M., Du, H., Wang, D., 2019. Mercury methylation by anaerobic microorganisms: a review. Crit. Rev. Environ. Sci. Technol. 49 (20), 1893–1936. https://doi.org/10.1080/10643389.2019.1594517.

Ma, J.-Y., Wang, S.-Y., Du, Y.-C., Wang, D.-X., Tang, A.-N., Wang, J., Kong, D.-M., 2022. "RESET" effect: random extending sequences enhance the trans-cleavage activity of CRISPR/Cas12a. Anal. Chem. 94 (22), 8050–8057. https://doi.org/10.1021/acs.analchem.2c01401.

Meng, M., Liu, H.W., Yu, B., Yin, Y.G., Hu, L.G., Li, Y.B., Chen, J.B., Shi, J.B., Jiang, G.B., 2021. Mercury inputs into eastern China seas revealed by mercury isotope variations in sediment cores. J. Geophys. Res. Oceans 126 (8) (://WOS:000690758000024).

Ooi, K.H., Liu, M.M., Tay, J.W.D., Teo, S.Y., Kaewsapsak, P., Jin, S., Lee, C.K., Hou, J., Maurer-Stroh, S., Lin, W., et al., 2021. An engineered CRISPR-Cas12a variant and DNA-RNA hybrid guides enable robust and rapid COVID-19 testing. Nat. Commun. 12 (1), 1739. https://doi.org/10.1038/s41467-021-21996-6.

Parks Jerry, M., Johs, A., Podar, M., Bridou, R., Hurt Richard, A., Smith Steven, D., Tomanicek Stephen, J., Qian, Y., Brown Steven, D., Brandt Craig, C., et al., 2013. The genetic basis for bacterial mercury methylation. Science 339 (6125), 1332–1335. https://doi.org/10.1126/science.1230667.

de Puig, H.; Lee Rose, A.; Najjar, D.; Tan, X.; Soenksen Luis, R.; Angenent-Mari Nicolaas, M.; Donghia Nina, M.; Weckman Nicole, E.; Ory, A.; Ng Carlos, F.; et al. Minimally instrumented SHERLOCK (miSHERLOCK) for CRISPR-based point-of-care diagnosis of SARS-CoV-2 and emerging variants. Sci. Adv. 7 (32), eabh2944. doi:https://doi.org/10.1126/sciadv.abh2944.

Regnell, O., Watras, C.J., 2019. Microbial mercury methylation in aquatic environments: a critical review of published field and laboratory studies. Environ. Sci. Technol. 53 (1), 4–19. https://doi.org/10.1021/acs.est.8b02709.

Selin, N.E., 2009. Global biogeochemical cycling of mercury: a review. Annu. Rev. Env. Resour. 34 (1), 43–63. https://doi.org/10.1146/annurev.environ.051308.084314.

Shao, J., Shi, J., Duo, B., Liu, C., Gao, Y., Fu, J., Yang, R., Jiang, G., 2016. Mercury in alpine fish from four rivers in the Tibetan plateau. J. Environ. Sci. 39, 22–28. https://www.sciencedirect.com/science/article/pii/S1001074215004209.

Tang, Y.D., Qi, L.J., Liu, Y.C., Guo, L.L., Zhao, R.J., Yang, M.T., Du, Y., Li, B.L., 2022. CLIPON: a CRISPR-enabled strategy that turns commercial pregnancy test strips into general point-of-need test devices. Angewandte Chemie-International Edition 61 (12). ://WOS:000749623400001.

Wang, X., Ye, Z., Li, B., Huang, L., Meng, M., Shi, J., Jiang, G., 2014. Growing rice aerobically markedly decreases mercury accumulation by reducing both Hg bioavailability and the production of MeHg. Environ. Sci. Technol. 48 (3), 1878–1885. https://doi.org/10.1021/es4038929.

Wang, G., Tian, W., Liu, X., Ren, W., Liu, C., 2020. New CRISPR-derived microRNA sensing mechanism based on Cas12a self-powered and rolling circle transcription-unleashed real-time crRNA recruiting. Anal. Chem. 92 (9), 6702–6708. https://doi.org/10.1021/acs.analchem.0c00680.

Wang, H., He, Y., Wei, J., Wang, H., Ma, K., Zhou, Y., Liu, X., Zhou, X., Wang, F., 2022. Construction of an autocatalytic hybridization assembly circuit for amplified in vivo MicroRNA imaging. Angew. Chem. Int. Ed. 61 (19), e202115489 https://doi.org/10.1002/anie.202115489.

Wu, Q., Wang, S., Li, G., Liang, S., Lin, C.-J., Wang, Y., Cai, S., Liu, K., Hao, J., 2016. Temporal trend and spatial distribution of speciated atmospheric mercury emissions in China during 1978–2014. Environ. Sci. Technol. 50 (24), 13428–13435. https://doi.org/10.1021/acs.est.6b04308.

Wu, Q., Hu, H., Meng, B., Wang, B., Poulain, A.J., Zhang, H., Liu, J., Bravo, A.G., Bishop, K., Bertilsson, S., et al., 2020. Methanogenesis is an important process in controlling MeHg concentration in rice paddy soils affected by mining activities. Environ. Sci. Technol. 54 (21), 13517–13526. https://doi.org/10.1021/acs.est.0c00268.

Zeng, M., Ke, Y., Zhuang, Z., Qin, C., Li, L.Y., Sheng, G., Li, Z., Meng, H., Ding, X., 2022. Harnessing multiplex crRNA in the CRISPR/Cas12a system enables an amplification-free DNA diagnostic platform for ASFV detection. Anal. Chem. https://doi.org/10.1021/acs.analchem.2c01588.

Zhang, H., Feng, X., Larssen, T., Shang, L., Li, P., 2010. Bioaccumulation of methylmercury versus inorganic mercury in rice (Oryza sativa L.) grain. Environ. Sci. Technol. 44 (12), 4499–4504. https://doi.org/10.1021/es903565t.

Zhang, L., Sun, R., Yang, M., Peng, S., Cheng, Y., Chen, C., 2019. Conformational dynamics and cleavage sites of Cas12a are modulated by complementarity between crRNA and DNA. iScience 19, 492–503. https://www.sciencedirect.com/science/article/pii/S2589004219302834.

Zhang, H., Wang, W., Lin, C., Feng, X., Shi, J., Jiang, G., Larssen, T., 2022. Decreasing mercury levels in consumer fish over the three decades of increasing mercury emissions in China. Eco-Environ. Health. 1 (1), 46–52. https://www.sciencedirect.com/science/article/pii/S2772985022000059.

Zhao, Y., Chen, F., Li, Q., Wang, L., Fan, C., 2015. Isothermal amplification of nucleic acids. Chem. Rev. 115 (22), 12491–12545. https://www.ncbi.nlm.nih.gov/pubmed/26551336.

Zhao, L., Meng, B., Feng, X., 2020. Mercury methylation in rice paddy and accumulation in rice plant: a review. Ecotoxicol. Environ. Saf. 195, 110462. https://www.sciencedirect.com/science/article/pii/S0147651320303018.